

# Functional Clustering: Identifying Strongly Interactive Brain Regions in Neuroimaging Data

Giulio Tononi, Anthony R. McIntosh,\* D. Patrick Russell, and Gerald M. Edelman

*The Neurosciences Institute, 10640 John J. Hopkins Drive, San Diego, California 92121;*

*\*Rotman Research Institute of Baycrest Centre, 3560 Bathurst Street, Toronto, Ontario M6A 2E1 Canada*

Received July 17, 1997

---

**Brain imaging data are generally used to determine which brain regions are most *active* in an experimental paradigm or in a group of subjects. Theoretical considerations suggest that it would also be of interest to know which set of brain regions are most *interactive* in a given task or group of subjects. A subset of regions that are much more strongly interactive among themselves than with the rest of the brain is called here a *functional cluster*. Functional clustering can be assessed by calculating for each subset of brain regions a measure, the *cluster index*, obtained by dividing the statistical dependence within the subset by that between the subset and rest of the brain. A cluster index value near 1 indicates a homogeneous system, while a high cluster index indicates that a subset of brain regions forms a distinct functional cluster. Within a functional cluster, individual brain regions are ranked at the center or at the periphery according to their statistical dependence with the rest of that cluster. The applicability of this approach has been tested on PET data obtained from normal and schizophrenic subjects performing a set of cognitive tasks. Analysis of the data reveals evidence of functional clustering. A comparative evaluation of which regions are more peripheral or more central suggests distinct differences between the two groups of subjects. We consider the applicability of this analysis to data obtained with imaging modalities offering higher temporal resolution than PET.** © 1998 Academic Press

---

## INTRODUCTION

Neuroimaging provides access to neural substrates of higher cognitive functions that are difficult to study in animal models. In most imaging studies, the aim is to determine whether certain brain regions are significantly more or less *active* than other brain regions by comparing activity values in different tasks or groups of subjects (Petersen *et al.*, 1988). Studies of this kind have provided fundamental data to indicate which brain regions are strongly activated in cognitive tasks

or compromised by pathological processes (Budinger, 1992; Heiss *et al.*, 1992). There is evidence, however, that higher cognitive functions require the rapid integration of information across several sensory and behavioral domains through reentrant interactions among widely distributed brain regions (Edelman, 1987, 1989; Tononi *et al.*, 1992, 1994). This suggests that it would be important to know which brain regions are most *interactive* in a given task or group of subjects (McIntosh and Gonzalez-Lima, 1994; Friston, 1994).

Imaging techniques such as PET and fMRI have only recently been employed to explore the functional interactions between different brain areas in a given task or group of subjects (Moeller and Strother, 1987; McLaughlin *et al.*, 1992; McIntosh *et al.*, 1994, 1996a; Friston, 1994). To characterize the joint interactions among many brain regions, rather than just the interactions between two regions at a time, multivariate measures of statistical dependence have been introduced (Tononi *et al.*, 1994, 1996; Friston *et al.*, 1996b). A basic question that needs to be asked of neuroimaging data even before characterizing the dynamics of neural interactions is whether they show evidence of *functional clustering*. A functional cluster can be defined as a set of elements that are much more strongly interactive among themselves than with the rest of the system, whether or not the underlying anatomical connectivity is continuous. The presence of functional clustering would indicate significant discontinuities in the interactions among brain regions. Such discontinuities could have important implications particularly because only signals exchanged within a functional boundary can be integrated. Their analysis may uncover important aspects of cognitive integration in the normal brain (McIntosh *et al.*, 1996b), as well as its breakdown in disorders showing symptoms of functional disconnection, such as schizophrenia and dissociative disorders (Edelman, 1989; Friston and Frith, 1995).

To address the issue of functional clustering explicitly, the present article introduces a measure, the *cluster index*, which relates the statistical dependence

within a subset of brain regions to that between that subset and the rest of the brain. A cluster index value near 1 indicates a system with no discontinuities, while a high cluster index indicates that a subset of brain regions forms a distinct cluster having functional boundaries with the rest of the brain. The procedures described here are aimed at determining whether a functional cluster is present, its composition, and whether that composition changes between tasks or subjects. Following a theoretical analysis, the applicability of these procedures is tested on a PET data set obtained from normal and schizophrenic subjects performing a set of cognitive tasks.

## THEORY

In cluster analysis, a cluster is loosely defined as a subset of elements that are cohesive among themselves but relatively isolated from the remaining elements (cf. Cormack, 1971; Gordon, 1980; Everitt, 1993). In terms of brain dynamics, a functional cluster can be defined as a subset of neural elements that are strongly interactive among themselves but weakly interactive with the rest of the system. This intuitive notion can be made precise and can be applied to imaging data by using multivariate measures of statistical dependence among neural elements. Two such measures, reviewed below, are integration (Tononi *et al.*, 1994) and mutual information (Papoulis, 1991): Integration measures the total statistical dependence among a subset of elements, while mutual information measures the statistical dependence between that subset of elements and the rest of the system. The ratio between integration and mutual information, or the *cluster index*, can thus serve as a measure of functional clustering. By calculating and ranking cluster indices for a large sample of subsets of a given system, it is possible to establish the presence of functional clusters, to determine cluster boundaries, to reveal the elements included in each cluster, and to obtain the ranking of elements by their mutual information within a cluster.

### Mutual Information and Integration

Consider a neural system  $X$  composed of a set of  $N$  neural elements  $\{x_j\}$  whose physiological activation is reflected by the activity value of a set of  $N$  voxels in an imaging data set. We assume that the activity of these elements is described by a stationary multidimensional stochastic process (Papoulis, 1991). The joint probability density function describing such a multivariate process can be characterized in terms of entropy and mutual information (Shannon and Weaver, 1949; Papoulis, 1991). Entropy and mutual information are used here purely in their statistical connotation; they can be thought of as the multivariate generalizations of variance and covariance in univariate statistics.

In the context of neuroimaging data comprising  $N$  voxels and  $M$  scans, entropy, integration, and mutual information can be visualized by thinking of the volume occupied by  $M$  points in an  $N$ -dimensional space, of which entropy provides a measure. If the  $N$  voxels are independent, the  $M$  points occupy a large volume in the  $N$ -dimensional space, and entropy is high. If there are constraints that enforce statistical dependencies among the voxels, the  $M$  points occupy a smaller volume. Integration measures such reduction in volume or entropy.

Consider a bipartition of the system  $X$  into a  $j$ th subset  $X_j^k$ , composed of  $k$  elements, and its complement  $X - X_j^k$ . If we indicate the entropy of the  $j$ th subset as  $H(X_j^k)$ , the mutual information (MI) between  $X_j^k$  and  $X - X_j^k$  is (Papoulis, 1991)

$$MI(X_j^k; X - X_j^k) = H(X_j^k) + H(X - X_j^k) - H(X). \quad (1)$$

The mutual information is zero if  $X_j^k$  and  $X - X_j^k$  are statistically independent; it is greater than zero otherwise.

The concept of mutual information can be generalized to express the deviation from independence among the  $N$  components of a system  $X$  by means of a single measure, which we have called integration,  $I(X)$  (Tononi *et al.*, 1994).  $I(X)$  is defined as the difference between the sum of the entropies of all individual components  $\{x_j\}$  considered independently and the entropy of  $X$  considered as a whole:

$$I(X) = \sum_{i=1}^N H(x_i) - H(X). \quad (2)$$

Thus, the integration  $I(X)$  represents a multivariate measure of the total amount of deviation from statistical independence within the system. Assuming that the system is isolated, or that the amount of correlated input it receives from outside is constant, the integration represents a measure of the total amount of interaction within the system. Note that  $I(X)$  is equal to the sum of values of the mutual information between parts resulting from the recursive bipartition of  $X$  down to its elementary components. In particular, by eliminating one component at a time,  $I(X) = \sum_{j=1}^{N-1} MI(x_j; [x_{j+1}, x_{j+2}, \dots, x_N])$ .

### Cluster Index

A "functional cluster" is a set of elements that are much more strongly interactive among themselves than with the rest of the system. To identify subsets of elements satisfying this requirement, a cluster index (CI) is defined for each subset  $i$  according to

$$CI(X_i^k) = I(X_i^k) / MI(X_i^k; X - X_i^k). \quad (3)$$

Thus, a cluster index near 1 indicates a subset of elements that are as interactive among themselves as with the rest of the system. A cluster index much higher than 1 indicates instead a subset of elements that are strongly interactive among themselves but weakly interacting with the rest of the system, i.e., a set of elements that corresponds to the notion of a functional cluster. Finally, a cluster index smaller than 1 indicates a subset of elements that are less interactive among themselves than with the rest of the system. It should be emphasized that the use of integration and mutual information as measures of statistical dependence, respectively inside and outside the cluster, has the virtue that both measures are multivariate and are sensitive to high-order moments of statistical dependence (Papoulis, 1991). A simple demonstration of the power of a cluster index thus defined is given in Appendix 1.

It is often assumed that, as is the case with PET data, the probability density function of  $X$  conforms to a multidimensional Gaussian. In that case, the system can be completely characterized by its covariance matrix (Jones, 1979), which is the  $N \times N$  symmetric matrix of covariances between all pairs of elements,  $\text{COV}(X)$ . The  $i$ th diagonal element of  $\text{COV}(X)$  is the variance of the  $i$ th element  $x_i$ , namely  $\sigma_i^2$ . Under these assumptions, the entropy of  $x_i$ ,  $H(x_i)$ , is given by  $H(x_i) = (1/2) \ln(2\pi e \sigma_i^2)$ , and the entropy of  $X$  is  $H(X) = (1/2) \ln[(2\pi e)^N |\text{COV}(X)|]$ , where  $|\cdot|$  is the determinant. In this context, integration reduces to  $I(X) = -0.5 \ln|\text{CORR}(X)|$ , where  $\text{CORR}(X)$  is the cross-correlation (normalized covariance) matrix of  $X$ .<sup>1</sup>

Note that, while the assumption of a multidimensional Gaussian probability density function simplifies the computation of entropy, integration, and mutual information, any nonlinear dependencies are discounted. Although the general formulation of a cluster index presented here is in principle sensitive to deviations from independence of any order, for the purpose of this paper only first order correlations will play a role.

One of the properties sought from the cluster index was the ability to make meaningful comparisons between different subsets, independent of subset size. The scaling of the integration and mutual information with subset size is not the same, however, even in the absence of functional clustering (see Fig. 1). In order to obtain a CI that was insensitive to subset size, the integration and mutual information were normalized by their respective averages as a function of subset size in an equivalent nonclustered, or homogeneous, system  $X_H$ :  $\text{CI}(X_i^k) = I_n(X_i^k)/MI_n(X_i^k; X - X_i^k)$ ; where  $I_n(X_i^k) =$

$I(X_i^k)/I(X_H^k)$ ,  $MI_n(X_i^k; X - X_i^k) = MI(X_i^k; X - X_i^k)/(MI(X_H^k; X - X_H^k))$ .  $X_H$  is a system the probability distribution function of which is also a multidimensional Gaussian of the same size  $N$  and total integration  $I(X)$ , but one that has a homogeneous correlation matrix (all pairwise correlations equal) and hence that is characterized by no functional clustering (see Appendix 2). To obtain the average integration  $\langle I(X_H^k) \rangle$  and mutual information  $\langle MI(X_H^k; X - X_H^k) \rangle$  at each subset size  $k$ , many such systems were sampled and analyzed (see Appendix 2). The average mutual information and integration as a function of subset size of one of the PET data sets discussed below, as well as of the equivalent homogeneous system, are shown in Fig. 1.

In order to assess the statistical significance of a given cluster index, a Student's  $t$  parameter,  $t_{\text{CI}}$ , was calculated by subtracting from each CI the mean value of the same null system used to provide normalization values and dividing by the standard deviation of this null population. It was found in null systems  $X_H$  that the mean cluster index was one for all subset sizes (hence permitting comparisons between cluster indices drawn from different subset sizes), but that the standard deviation of the distribution varied with subset size (see Fig. 2). In order to compensate for this, the  $t_{\text{CI}}$  was calculated using the mean and standard deviations by subset size in the null population (see Appendix 2 for details). This statistic can be calculated for a specified number of null systems and used to provide the probability of obtaining a given data  $t_{\text{CI}}$  under the null hypothesis, thus providing a rigorous statistical interpretation to cluster index measurements.

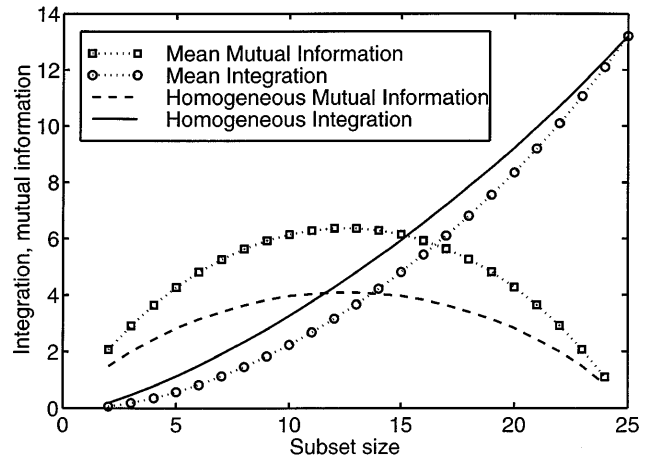


**FIG. 1.** Mean values of integration and mutual information as a function of subset size for two different systems. The symbols indicate the average integration (circles) and mutual information values (squares) of a PET imaging data set (shown in Fig. 5A); the average integration (solid line) and mutual information values (dashed line) of an equivalent homogeneous system are shown for comparison. The latter are used as the normalization values in the CI calculation of the given PET-data system.

<sup>1</sup> In the context of canonical correlation analysis, mutual information between  $X_i^k$  and  $X - X_i^k$  can be shown to correspond to  $MI(X_i^k; X - X_i^k) = \sum_{j=1}^k (1 - r_j^2)$ , where  $r_j$  is the  $j$ th canonical correlation between  $X_i^k$  and  $X - X_i^k$ . The latter correspondence was pointed out by an anonymous reviewer.

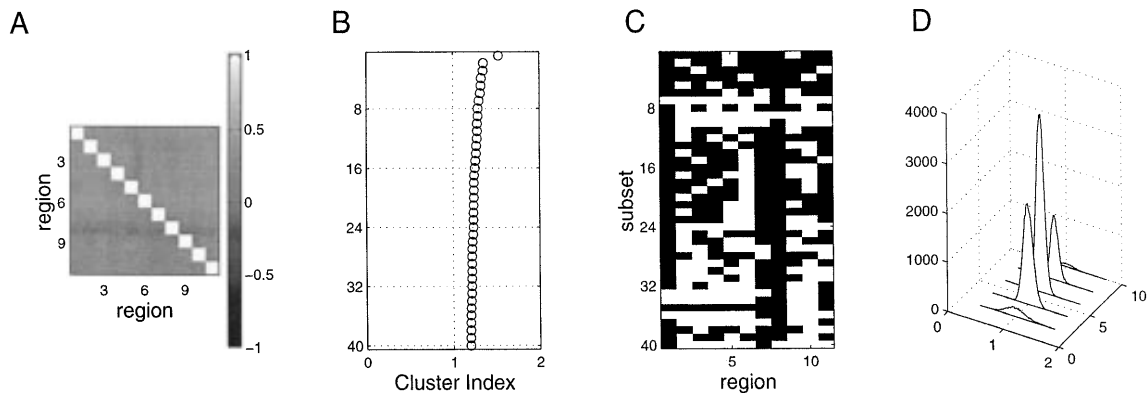


**FIG. 2.** Cluster index analysis for a simulated homogeneous system. The system was drawn from an 11-dimensional Gaussian distribution of average correlation coefficient 0.32 between all pairs of elements (regions). (A) The correlation matrix resulting from one such sampling. (B) The 40 highest cluster index values, indicated by open circles. (C) Subset matrix. Schematic representation of the composition of the subsets corresponding to the CI values in (B). White indicates that an element is part of the subset; black means that it is not. (D) Histogram of CI values of 100 systems drawn from same distribution as was A; CI distributions are shown separately for subset sizes 2, 4, 6, 8, and 10.

### Cluster Index Analysis

To demonstrate the properties of the cluster index, two different systems composed of  $N = 11$  elements were generated, both of which consisted of 1000 samples drawn from an 11-dimensional Gaussian probability distribution function (see Appendix 2). The covariance matrix characterizing the probability distribution function for the first system was homogeneous, with an average correlation coefficient of 0.32 between all pairs of elements. Figure 2A shows the sampled correlation matrix, which is flat except for statistical fluctuations. This corresponds to a homogeneous system, in which there are no boundaries among the 11 elements. In the second system, the average covariance values de-

creased linearly from a maximum at element 1 to zero at elements 7 to 11. Hence elements 1–6 formed a distinct cluster having a functional boundary with the other elements (Fig. 3A).

The main outcome derivable from cluster index analysis is a list of the subsets of a system ranked by their CI values. The highest CI values for all the subsets of the homogeneous system, ranked in ascending order regardless of their subset size  $k$ , are shown in Fig. 2B. The composition of the subsets corresponding to each CI is schematically represented in Fig. 2C. CI values close to 1 indicate that this system does not contain a cluster boundary; i.e., it is homogeneous. Figure 2D displays the distribution of the CI values resulting from 100

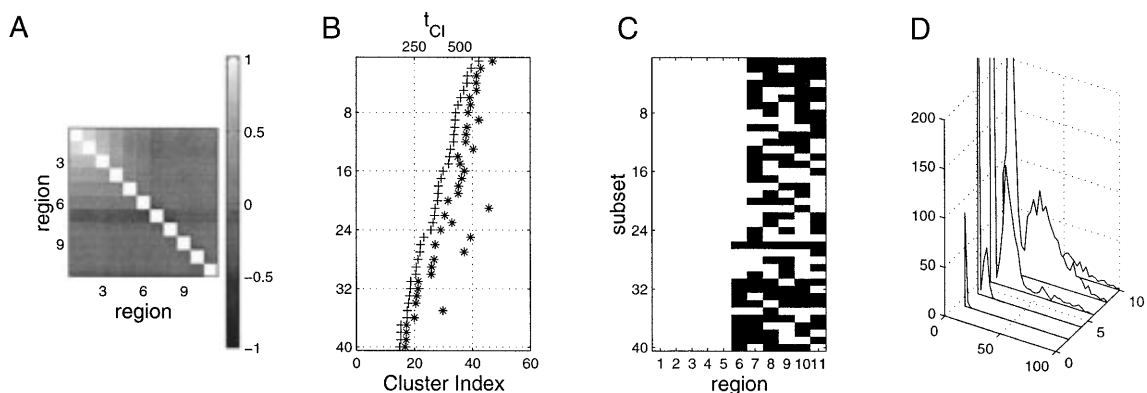


**FIG. 3.** Cluster index analysis for a simulated system containing a functional cluster. The system was drawn from a Gaussian distribution with elements 1–6 forming a cluster with correlation decreasing linearly from element 1 to element 6. (A) Sampled correlation matrix. (B) 40 most significant subsets ranked by value of  $t_{CI}$ , indicated by the plus sign (scale on the upper abscissa). This is a Student's  $t$ -like parameter,  $t_{CI}$ , which expresses a given CI in terms of the number of standard deviations that it lies from the mean of subset size  $k$  of the equivalent homogeneous system. CI values are indicated by the adjacent asterisks (scale on the lower abscissa). The asterisk indicates that in Monte Carlo simulations of the equivalent homogeneous system subsets of the same size yielded CI values that were equal or higher with  $P < 0.001$ . (C) Corresponding subset compositions. Elements 1 to 6 constitute a functional cluster with  $CI = 47$ . (D) CI histograms of subset sizes 2, 4, 6, 8, and 10 drawn from 100 sampled systems.

systems sampled from the same distribution as was Fig. 2A. The CI distribution has been separately histogrammed by subset size for  $k = 2, 4, 6, 8,$  and  $10$ . Notice that the distributions are all centered around  $CI = 1$  due to the normalization of CI across subset sizes. The absolute significance of a given CI value can be established by assessing the probability of finding subsets of the same size with equal or higher CI values in Monte Carlo simulations of equivalent homogeneous systems (see Appendix 2). If the highest CI values for the system under consideration are higher than those expected in a significant number of corresponding homogeneous systems ( $P < 0.01$ ), it is likely that the system contains one or more functional clusters.

This procedure is illustrated for the system shown in Fig. 3A, that was designed to contain a functional cluster. Figure 3B shows the most significant CIs ranked according to their  $t_{CI}$  values, which are also plotted. The most relevant information is contained at the top of the matrix, which identifies the subsets with the highest CI values. Figure 3C shows the corresponding subsets, and Fig. 3D contains the CI distribution histograms of 100 systems, as in Fig. 2D. The most significant subset in Fig. 3B has a CI value of 47 and, as shown by Fig. 3C, it consists of elements 1–6, the elements with nonzero average correlation. The 20 next most significant subsets all consist of elements 1–6 with various additions from the remaining elements 7–11, indicating that the second system contains a cluster with distinct boundaries. Note that cluster boundaries can be organized hierarchically, in that small, tight functional clusters can be found within a large cluster. In other instances, there may be two or more distinct clusters, which can be overlapping or not. In general, it is possible to span a continuum between a cluster with sharp boundaries and a completely homogeneous system.

Practically, the procedure just described can be applied exhaustively only to systems composed of at most one or two dozen elements because the number of subsets to be considered increases as  $2^{N-1} - 1$ . When dealing with larger systems, a random sampling of subsets at each level (e.g., 10,000 samples per level) provides an initial, nonexhaustive cluster matrix. An optimization for CI can then be performed by appropriately permuting the subsets with the highest CI (cf. Everitt, 1993, for optimization procedures in cluster analysis). In most cases, this procedure rapidly identifies the subsets with the highest CI among millions of possibilities. Alternatively, or if the data are noisy, it is possible to treat the cluster matrix statistically. The subsets having significant CI values can be cross-correlated, weighted by their CI. The eigenvector of this correlation matrix having the largest eigenvalue will

indicate a grouping of units that is likely to represent the composition of a functional cluster (data not shown).

### Ranking the Elements within a Functional Cluster

The values of CI only indicate whether or not there are cluster boundaries within the system under consideration. In the absence of a boundary, two possibilities need to be considered. If the system under consideration has a high value of integration  $I(X)$ , it may be part of a larger functional cluster. Its boundaries can then be revealed by applying the present analysis to a larger collection of elements. If instead the system under consideration has a low value of  $I(X)$ , it is too loosely coupled for functional clustering to emerge. Within the boundaries of a given functional cluster, a simple one-dimensional ranking of the individual elements can be obtained by considering the MI of each element with the rest of the cluster. Elements with a higher value of MI can be considered to lie at the center of the cluster, while elements with lower values of MI can be considered to lie at its periphery. The identified cluster boundaries and the one-dimensional ranking of elements within a cluster can then be used to reorder rows and columns of the covariance matrix to reveal its structure. For the system with cluster boundaries, within the functional cluster containing elements 1 to 6, the ranking by MI values identifies a center (element 1) and a periphery (elements 5–6, Fig. 4).

Once the presence and composition of a functional cluster have been established, several multivariate approaches can be considered to characterize further the nature of the interactions within the functional cluster. Among such approaches are principal component analysis (Moeller *et al.*, 1987; Friston, 1994), multidimensional scaling (Goldberg *et al.*, 1989; Friston *et al.*, 1996a), path analysis (McIntosh and Gonzalez-Lima, 1994), and the calculation of the complexity, or integration of information, within the cluster (Tononi *et al.*, 1994).

### PET DATA SET

The procedure for identifying and characterizing functional clusters introduced here was tested on several simulated data sets of known structure (multiple clusters, fuzzy boundaries, subclusters linked by bridging elements, etc.). In all these cases, the procedure was able to detect functional clusters in a way that conformed with the known structure as well as with intuition (data not shown). The potential usefulness of this approach lies, however, in applying it to imaging data having an unknown structure.

As an example, we have analyzed the results of a PET study with chronic schizophrenics ( $N = 8$ ; average age = 37) and age- and sex-matched controls ( $N = 8$ ; average age = 36) performing three simple cognitive

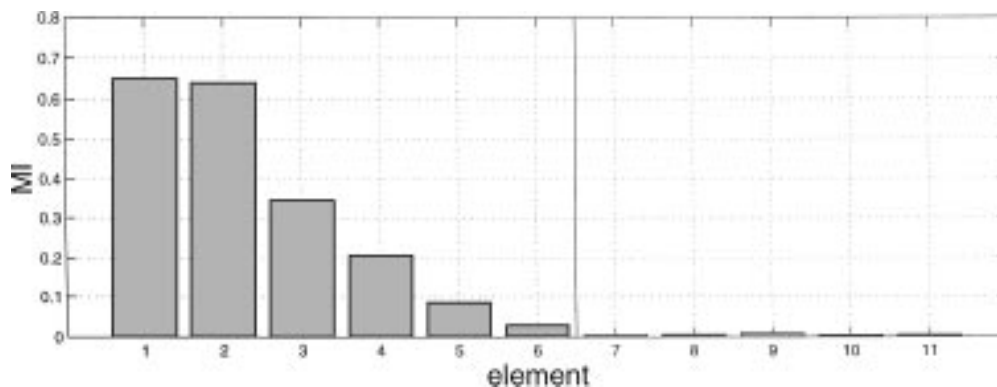


**FIG. 4.** Rankings of the elements for the simulated system containing a functional cluster. The elements are ranked based on their mutual information with the functional cluster to which they belong. The vertical line indicates the border of the functional cluster identified by the cluster index analysis shown in Fig. 3B (corresponding to the subset at the top of the matrix in Fig. 3C).

tasks. This data set was chosen because no differences between schizophrenics and controls had been found when solely analyzing activity measures by statistical parametric mapping (SPM; Friston *et al.*, 1995b; unpublished results). The schizophrenic patients had been diagnosed according to DSM-IV criteria and were all medicated and stable.

The three tasks were as follows. In the first condition, subjects presented with an arrow on a video screen were asked to press a button on a computer mouse that was on the same side as that to which the arrow pointed (Arrow task). The second condition consisted of presentations of single words (nouns), and the task was to indicate, by pressing the mouse button, whether the word contained the letter “a” (Letter task). Words were also presented in the final condition, but the subjects were asked to judge whether the word represented a living or nonliving thing (Living task). The first condition was scanned once, conditions two and three were scanned twice.

Images were acquired over 1 min using a fast dynamic  $^{15}\text{O}$  technique with a GE Medical Systems 2048-15 scanner. Raw PET images were corrected for interscan movement using a rigid body transformation and then registered to a common stereotaxic template image using a 12 parameter affine transformation followed by a nonlinear 2-D transformation using basis functions (SPM95, Friston *et al.*, 1995a). Voxel values within a scan were ratio-adjusted using the mean of that scan for each subject. Since the correlations used in the analysis of functional clustering were computed across all scans, the voxels were further adjusted by subtracting from each voxel value the mean of that voxel within subject. This expresses the voxel value as the deviation from that subject’s grand mean, i.e., task variation, and eliminates constant individual differences that would obscure the covariance structure. Voxel-by-voxel comparisons were conducted to identify task-related main effects that were common to both

groups as well as task effects that differed between groups (group-by-task interactions). There were no voxels that showed a significant group-by-task interaction.

A set of 25 voxels was then chosen based on peak task-related differences identified in the SPM analysis (Table 1). Thirteen voxels showed differences between the Arrow task and the other two conditions, 6 showing greater regional cerebral blood flow (rCBF) and 7 showing lower rCBF in the Arrow task. The remaining 12 voxels showed differential rCBF between the Letter and the Living tasks, half showing greater rCBF and half showing lower rCBF during the Living task relative to the Letter task. For each group of subjects, a covariance matrix was obtained for these voxels using the 8 subjects  $\times$  5 scans as the source of variance (note that the analysis of this data set can be applied only to subsets of  $\leq 35$  pixels because of the limited number of degrees of freedom, i.e., 40 different values for each voxel, minus the 5 mean corrections).

A second set of voxels was chosen using a voxel-of-interest (VOI) template that sampled voxels based on the stereotaxic template. After resampling and stereotaxic normalization, the voxel dimensions were  $2 \times 2 \times 4$  mm. VOIs were placed such that there was minimal influence from spatial autocorrelation induced by image smoothing (estimated size of the spatial autocorrelation function was about 6 mm in plane for this data set). From the resulting 270 voxels we chose a set of 11 that could potentially yield a high CI. Six voxels were chosen from a region extending from left inferior parietal to superior temporal into middle prefrontal cortex, 2 from right dorsal occipital cortex, 2 from right inferior prefrontal cortex, and 1 from striate cortex. It should be noted that the choice of this second set of voxels is meant only as a demonstration of functional clustering using empirical data and the significance of the analysis does not extend beyond that purpose.

**TABLE 1**

Local Maxima for Regions Showing Task-Related Changes in rCBF Common to Both Controls and Schizophrenics as Identified by SPM ( $P < 0.001$  uncorrected)

| Areas             | X   | Y    | Z   | Task differences        |
|-------------------|-----|------|-----|-------------------------|
| Ra24I             | 22  | 24   | 16  | Letter > Living         |
| Ra18 <sub>1</sub> | 38  | -60  | -8  | Letter > Living         |
| La18 <sub>1</sub> | -42 | -86  | 0   | Letter > Living         |
| La19d             | -22 | -60  | 36  | Letter > Living         |
| Ra6               | 22  | -10  | 40  | Letter > Living         |
| Ra19d             | 24  | -62  | 32  | Letter > Living         |
| La47              | -28 | 22   | 0   | Living > Letter         |
| Ra22 <sub>1</sub> | -52 | -42  | 4   | Living > Letter         |
| Ra22 <sub>2</sub> | -58 | -4   | -4  | Living > Letter         |
| La18 <sub>2</sub> | -42 | -60  | -8  | Letter > Living         |
| La22 <sub>2</sub> | -54 | -30  | -4  | Living > Letter         |
| Ra46              | 30  | 45   | 0   | Living > Letter         |
| Ra18 <sub>2</sub> | 42  | -60  | 8   | Arrow > Letter + Living |
| Ra21              | 44  | -4   | -4  | Arrow > Letter + Living |
| Ra24m             | 6   | 44   | 0   | Arrow > Letter + Living |
| Ra45              | 40  | 38   | 8   | Arrow > Letter + Living |
| La21              | -40 | -10  | -4  | Arrow > Letter + Living |
| La22 <sub>1</sub> | -60 | -60  | 4   | Arrow > Letter + Living |
| Ra40              | 54  | -30  | 24  | Arrow > Letter + Living |
| La32              | -14 | 18   | 40  | Letter + Living > Arrow |
| La17v             | -8  | -102 | -12 | Letter + Living > Arrow |
| Ra17v             | 10  | -82  | -4  | Letter + Living > Arrow |
| La6               | -38 | -4   | 32  | Letter + Living > Arrow |
| La44              | -56 | 8    | 28  | Letter + Living > Arrow |
| La9               | -52 | 22   | 24  | Letter + Living > Arrow |

*Note.* Coordinates and area labels are in reference to the stereotaxic atlas of Talairach and Tournoux (1988) (l, lateral; m, medial; d, dorsal; v, ventral; R, right; L, left. The rightmost column indicates the tasks for which the rCBF in that location was different (see text for task description).

### Cluster Index Analysis

The cluster index analysis for the first set of 25 voxels of the controls is shown in Fig. 5A, and that for the second set of 11 voxels is shown in Fig. 5B. In Fig. 5A, low CI values indicate that there are no subsets forming a functional cluster. Since the voxels were chosen depending on their contribution to the tasks at hand, and given the limited number of voxels analyzed, this result suggests that all 25 voxels are strongly interacting among themselves, as further evidenced by the high value of their average correlation coefficient (absolute value 0.32). In other words, they are all part of the same functional cluster, which presumably includes many more elements. In Fig. 5B, by contrast, it appears that for the second set of voxels there is a clear-cut cluster boundary between the voxels sampled from the left hemisphere and those sampled from the other regions. In this case, it appears that these two subsets of brain regions are functionally disconnected, as might be anticipated given the selection of voxels.

The cluster index analyses for the first and second set of voxels of the schizophrenics group are shown in Figs.

6A and 6B, respectively. Neither of the voxel sets show a clear boundary indicative of functional clustering. The absence of a cluster boundary in the second data set of schizophrenics can be attributed to the presence of small but stable covariances between the left hemisphere voxels and the other five voxels. In the first set of voxels, there is no major difference in terms of cluster boundaries between controls and schizophrenics. As shown below, however, the ranking of the elements within each cluster differs between the two groups.

### Assessing Differences in Within-Cluster Ranking

The location of the set of voxels selected through SPM analysis is shown in Fig. 7. The voxels are color-coded according to the strength of their statistical dependence, i.e., their MI values, with the rest of the cluster for controls (Fig. 7A) and schizophrenics (Fig. 7B). The ranked MI values between each voxel and the rest of the cluster are shown in Fig. 8A for controls and in Fig. 8B for schizophrenics.

The two rankings can be compared through an equivalent of an image subtraction procedure. The MI values obtained for the schizophrenics were subtracted from those obtained for the controls on a region-by-region basis. This produces a diagram (Fig. 8C) which displays the positive or negative difference in MI between the two groups for each brain region within the functional cluster. For five areas this difference achieved statistical significance as assessed by a random permutation test (Edgington, 1980). The permutation test assesses the degree to which the observed differences in MI are due to the group assignment for each subject's data. The data were randomly re-assigned 500 times to each group, the MI computed with the new assignment, and at each permutation the difference in MI was assessed for each voxel. Left premotor area 6 ( $P = 0.006$ ), right dorsal area 19 ( $P = 0.055$ ), left area 18 ( $P = 0.06$ ), and right area 40 ( $P = 0.034$ ) had higher MI values for controls, while left area 44 ( $P = 0.074$ ) had a higher value of MI for schizophrenics. Additional statistical rigor could be obtained by correcting the chosen statistical threshold for multiple comparisons based on the number of elements within the cluster that are assessed for differences in MI ranking. Using the overly conservative Bonferroni correction, premotor area 6 would remain significant. Thus, in contrast to activation values, the functional interactions within the cluster of brain areas involved in the cognitive tasks evaluated in this study differ significantly between controls and schizophrenics.

### DISCUSSION

We have described a procedure for determining whether imaging data reveal evidence of functional

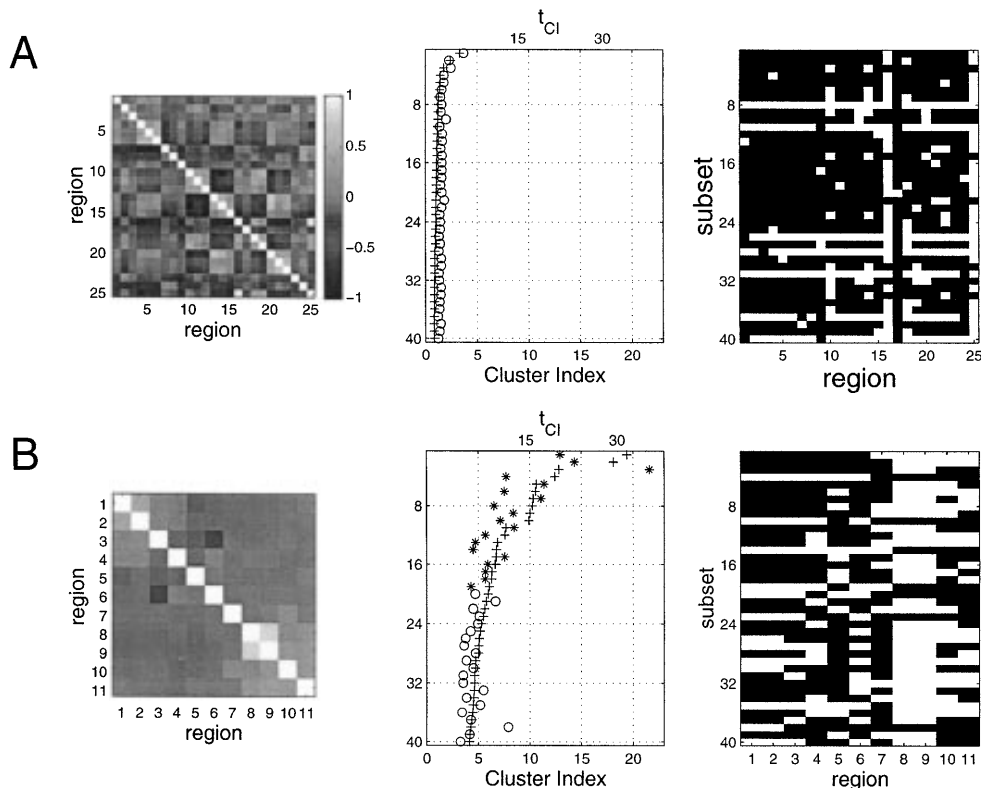


**FIG. 5.** Cluster index analysis for a PET data set from control subjects performing a set of cognitive tasks. (A) Activity values for 25 voxels chosen on the basis of peak task-related differences as determined by SPM analysis. (Left) Covariance matrix, (middle) highest cluster index values ranked by value of  $t_{CI}$ , (right) corresponding subsets. CI values are indicated by open circles or by a star if they reached significance in Monte Carlo simulations.  $t_{CI}$  values are indicated by the plus sign. Note that no CI value reached significance, suggesting that all voxels are part of the same functional cluster. (B) Activity values for 11 voxels chosen to illustrate cluster boundaries. Voxels 1–6 were selected from a region extending from left inferior parietal to superior temporal into middle prefrontal cortex, voxels 7–8 from right dorsal occipital cortex, voxels 9–10 from right inferior prefrontal cortex, and voxel 11 from striate cortex. As is evident also from the reordered covariance matrix, the highest CI values reached significance, suggesting that voxels 7 to 11 and 1 to 6 are part of two separate functional clusters.

clustering, i.e., evidence that certain subsets of brain regions interact much more strongly among themselves than with the rest of the brain. The procedure allows the establishment of the presence, composition, and boundaries of one or more functional clusters in a given task or group of subjects. It also permits ranking of brain regions within a cluster in terms of the strength of their statistical dependence. After demonstrating the procedure with synthetic models, a data set obtained in a PET study of schizophrenic patients was analyzed as an example. In what follows, we discuss the rationale for introducing such a procedure and we examine its relationships to other methods of data clustering. Finally, we briefly consider the results of the analysis of the PET data set.

### Functional Clustering: A Preliminary Step in the Analysis of Neural Interactions

While many kinds of multivariate analyses can be applied to imaging data in order to characterize neural interactions, we propose here that an important first

step should be the evaluation of functional clustering in the data. Such evaluation can aid in selecting, from the large set of voxels in imaging data sets, subsets of brain regions that stand out in terms of the strength of their interactivity, much as traditional approaches are used to select brain regions that stand out in terms of their activity.

Several considerations suggest that, in both physiological and pathological conditions, subsets of brain regions may transiently interact much more strongly among themselves than with the rest of the brain. This would lead to the emergence of functional boundaries despite the widespread connectivity that links all brain regions (Tononi and Edelman, in press). For instance, the presence of such functional boundaries is indicated by several manifestations of neurological disconnection syndromes (Geschwind, 1965), as well as by psychiatric conditions such as schizophrenia (Bleuler, 1911) and dissociative disorders (Lynn and Rhue, 1994). In the normal brain, while many brain regions are active in the control of cognition and behavior, only a subset of active neuronal groups is directly correlated with con-

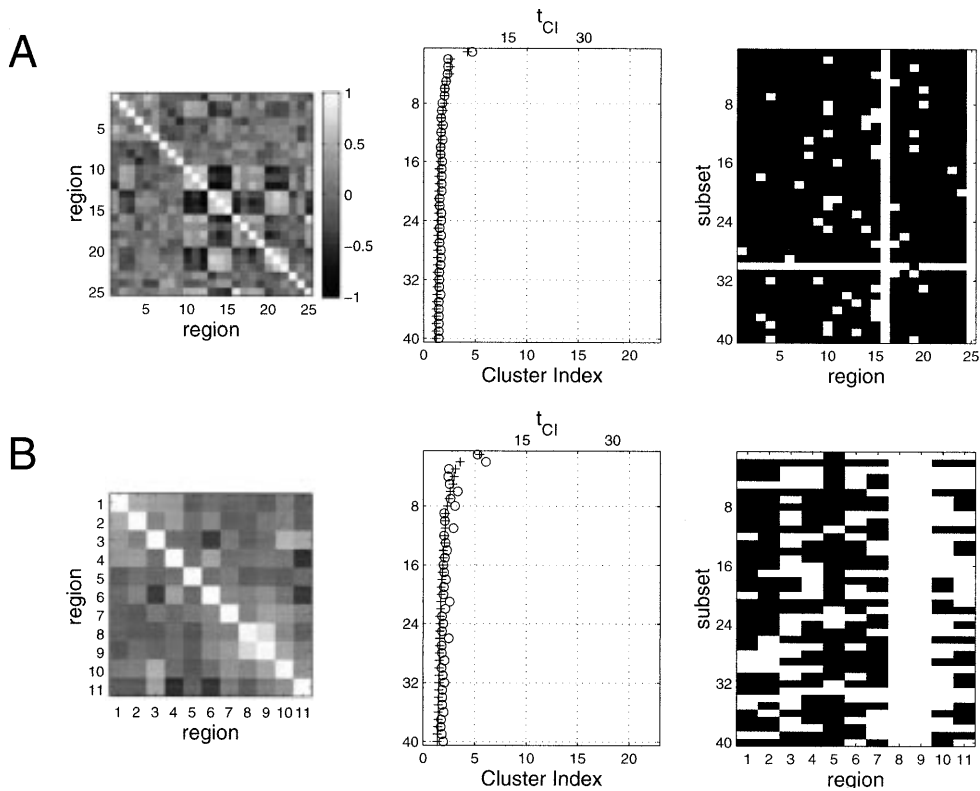


**FIG. 6.** Cluster index analysis for a PET data set from schizophrenic subjects performing a set of cognitive tasks. (A) Activity values for 25 voxels chosen on the basis of peak task-related differences as determined by SPM analysis. (B) Activity values for 11 voxels chosen to illustrate cluster boundaries. Panels as in Fig. 5. Note that no CI value reached significance.

scious experience (e.g., Leopold and Logothetis, 1996; Tononi *et al.*, in press). This suggests that, above and beyond the activity levels of such neuronal groups, critical differences with respect to stimulus awareness may be the strength, duration, and stability of their interactions within a distributed functional cluster (Tononi and Edelman, in press). The rapid and stable integration within a single functional entity of information obtained from many different sources, which is achieved by processes of reentry, is a central aspect of our cognitive abilities (Edelman, 1987; Tononi *et al.*, 1992). Signals integrated within a functional cluster are rapidly distributed to all its composing subsets and can thus simultaneously influence many aspects of brain function (Tononi *et al.*, 1992, 1994, 1996). Signals that are not integrated within a functional cluster are not globally distributed and can influence brain function only in a local and indirect manner. Finding experimental evidence for functional clustering in the brain would obviously have significant implications for our understanding of brain function.

From a practical point of view, several descriptive statistical techniques can be used to find evidence of functional clustering in imaging data in an expedient way. For instance, both principal component analysis (PCA), factor analysis (FA), independent component

analysis (ICA), and multidimensional scaling (MDS) can be used to facilitate the identification of clusters in data (Moeller *et al.*, 1987; Goldberg *et al.*, 1989; McLaughlin, *et al.*, 1992; Friston, 1994; McKeown *et al.*, 1997). However, it is well known that while PCA and related approaches may be useful in identifying important relationships within the data, there is no guarantee that PCA can find the clusters in multidimensional space that correspond to the intuitive notion of a cluster. In fact, PCA is not necessarily the better way for displaying the separation between groups or tasks, and it is not designed to search for structure but rather to summarize a large number of dimensions (Chang, 1983; Sneath, 1980; Widaman, 1993). Inasmuch as metric MDS is closely related to PCA (Cox and Cox, 1994), the same considerations apply to the former procedure. Both procedures can be profitably employed, as suggested earlier, in a preliminary analysis of the data to provide a good starting point for optimization.

The approach presented here aims at determining functional clustering directly by defining a cluster in terms of intrinsic vs extrinsic statistical dependencies and by examining a large number of candidate subsets in a data set. Although no universally accepted definition of a cluster exists in the statistical literature (Everitt, 1993; Arabie *et al.*, 1996), it is generally

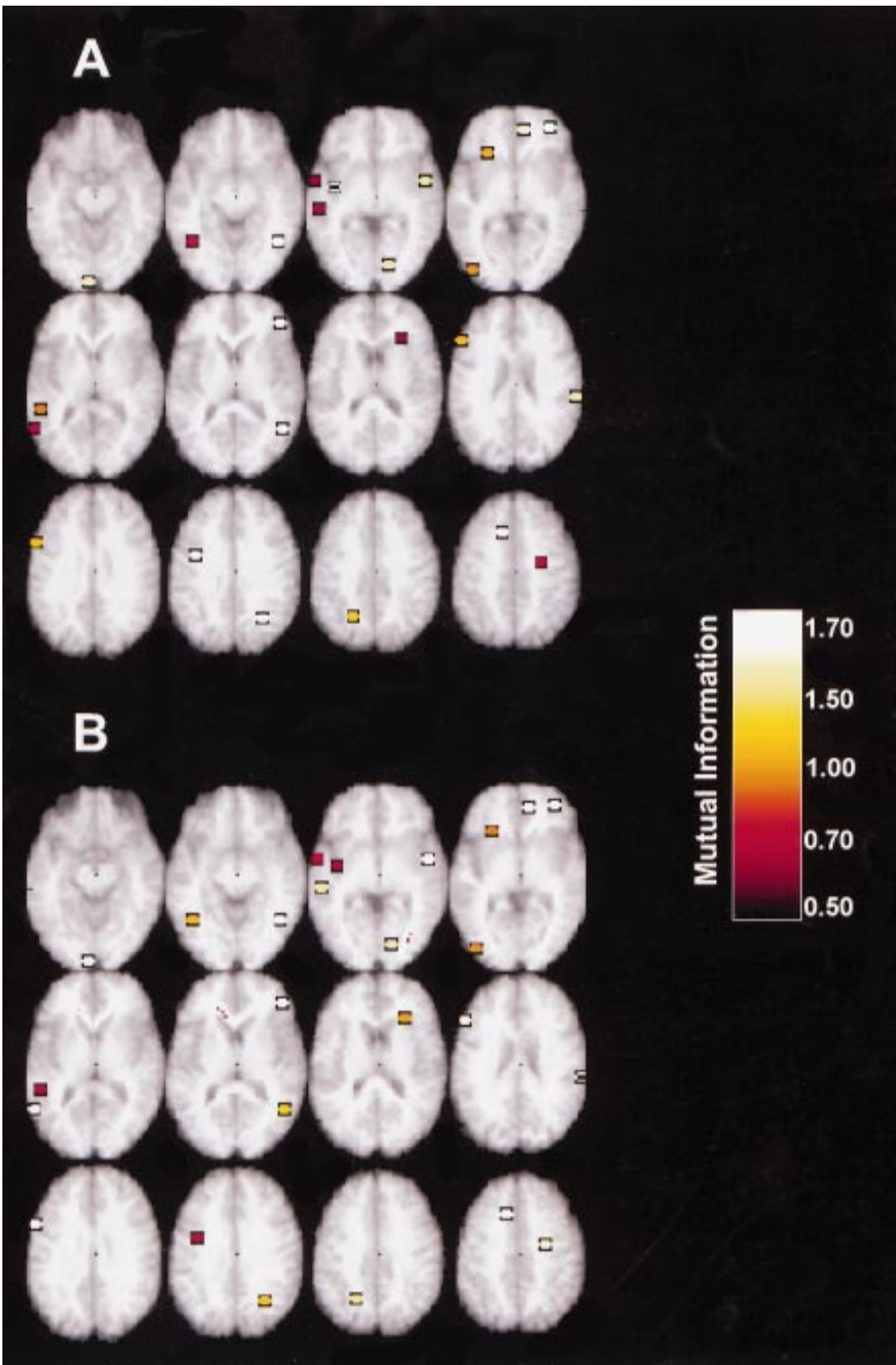


**FIG. 7.** Image of the set of 25 voxels identified by SPM analysis weighted by their mutual information within the functional cluster. Voxels are colored from black (lowest), through red and yellow to white (highest) depending on their mutual information with the rest of the functional cluster as indicated by the color scale on the right of the figure. (A) ranking for the controls; (B) ranking for the schizophrenics. The

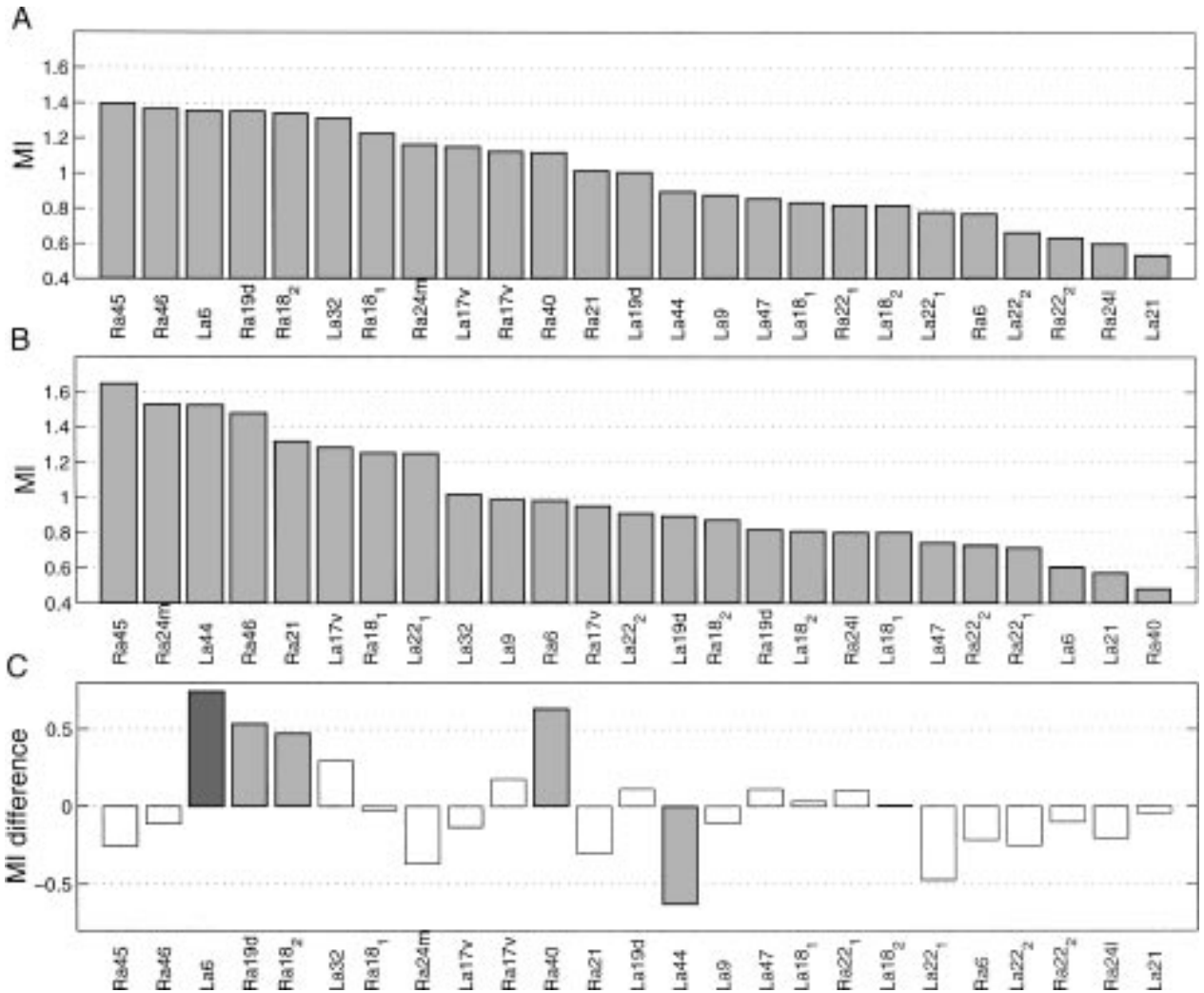


**FIG. 8.** Rankings of the 25 voxels identified by SPM analysis based on their mutual information within the functional cluster. (A) Controls, (B) schizophrenics. Voxels are ordered according to their mutual information with the rest of the system with labels as indicated in Table 1. (C) Difference in MI between controls and schizophrenics on a region-by-region basis. The difference is indicated by solid bars and voxel ordering is that of the control group. Shaded bars are voxels where the difference in MI was statistically significant as assessed through permutation tests assignment (see text for full explanation of this test). Bars shaded black are significant at  $P < 0.01$  and those shaded gray are significant at  $P < 0.1$ . Area abbreviations on the X-axis are the same as in Table 1.

agreed that a cluster should be defined in terms of internal cohesion and external isolation (cf. Cormack, 1971; Gordon, 1980). The cluster index developed here is based on integration as a measure of intrinsic statistical dependency within a subset of elements (internal cohesion) and on mutual information between that subset and its complement as a measure of extrinsic statistical dependency (external isolation). As a measure of similarity for clustering, mutual informa-

tion (with its derivatives) has the advantages of being multivariate, of being directly related to functional interactions, and of being sensitive to linear as well as nonlinear interactions. The enumerative procedure used here for the determination of functional clustering in a data set is related to various approaches in the context of cluster analysis, especially to the divisive enumerative procedure described by Chandon and Pinson (1981; cf. Kaufman and Rousseeuw, 1990). Although computa-

voxels are placed on a single structural MRI that conforms to the standard atlas space (left is left in the images). Mislocation of certain voxels to white matter represents an artifact of registering the low resolution PET coordinates onto the higher resolution MR. Slices proceed from ventral to dorsal going left to right columns and top to bottom rows (planes are located at Z coordinates: -12, -8, -4, 0, 4, 8, 16, 24, 28, 32, 36, 40 with reference to the Talairach and Tournoux atlas).

tionally expensive, an enumerative procedure is theoretically a satisfactory way of establishing the presence of clustering without bias. Depending on the specific application, faster clustering procedures can also be considered (Everitt, 1993).

### Application to Functional Neuroimaging

The PET data set considered here was not collected for the purpose of examining functional clustering and it is therefore to be expected that it presents several limitations. Perhaps the most important restriction is the limited number of degrees of freedom available due to the limited number of PET scans and subjects. This constrained the analysis of functional clustering to subsets of  $<35$  voxels. Another limitation is the source of variance in this study, which was variance among subjects and conditions as opposed to variance within a subject and within a task. The latter variance reflects how brain regions exchange signals in real time, but its calculation requires much higher temporal resolution. A useful feature of PET data is that, partly because of postacquisition processing, to a large degree they conform to multidimensional Gaussian assumptions. This makes the determination of CI values computationally convenient, but it does not exploit the power of measures such as integration and mutual information to detect nonlinear interactions. Finally, it should be kept in mind that the present analysis of functional clustering can explore only the statistical dependencies among brain regions. Distinguishing between statistical dependence and causal interaction requires additional assumptions or experimental manipulations.

Despite these limitations, the present analysis allowed us to draw some encouraging conclusions. In some cases, the limited number of brain regions considered here were shown to be part of the same functional cluster. These brain regions were selected because they showed significant task-related activity changes, and it is probably safe to assume that they may be part of a larger functional cluster. In other cases, it was possible to find evidence of a functional boundary, with certain sets of voxels belonging to one functional cluster and another set to a different cluster. In both instances, the present findings lend themselves to a physiologically meaningful interpretation. The voxels belonging to the same cluster were all functionally involved in the tasks studied while the voxels belonging to separate clusters were presumably functionally unrelated. Furthermore, it is possible to rank the regions belonging to a functional cluster in terms of the strength of their interaction with the rest of the cluster, thus identifying regions that are more central and others that are more peripheral in the many-to-many interactions that constitute a functional cluster. There can be significant differences in the ranking of certain brain regions between groups of subjects, as seen here for schizophrenics and con-

trols. Finally, boundaries between different functional clusters, as well as differences in the ranking within a cluster, can be present despite the absence of any difference in activation.

An examination of the same data sets with commonly used clustering methods was also performed, using both hierarchical and partitioning algorithms (e.g., *k*-means algorithm, with 2 to 5 groups). The comparison revealed that clusters identified through the present procedure were often reflected in the structure of dendrograms obtained from certain hierarchical algorithms (e.g., single-linkage clustering on Euclidean distances). However, different structures were obtained using different linkage methods, and deciding the appropriateness of one method over the other or testing for the significance of specific clusters becomes a serious problem. A partitioning algorithm (*k*-means, 2 to 5 groups) also found clusters that were broadly consistent with those identified by the present approach. This is expected given that the use of an integration/mutual information metric instead of the usual distance measures becomes less critical under the assumption of a multidimensional Gaussian distribution. By its own nature, however, the partitioning algorithm also found clusters when there were none. While the significance of the structure extracted by partitioning algorithms could also be tested against homogeneity or unimodality, a comparison of different clustering methods was not the purpose of the present paper. The topic of probability models and hypothesis testing in partitioning clustering analysis is analyzed in detail in Bock (1996).

The use of experimental protocols aimed at probing the presence and extent of functional clustering in the working brain, together with imaging methodologies offering higher temporal resolution, such as fMRI and topographic EEG and MEG, should overcome many of the technical limitations inherent in the present data set. Calculation of CI values and the accompanying descriptors could complement activation analyses such as SPM by sorting activated and deactivated regions into meaningful functional clusters. A procedure similar to the one employed here for group-related differences would be useful in the analysis of task-related differences in the organization of functional clusters. This would aid in determining whether a change in activity of particular regions between tasks is due to a reordering of areas within a cluster, or to a shift to an entirely different functional cluster. In addition, the use of faster imaging methodologies should make it possible to evaluate the dynamic occurrence and significance of functional clustering in the brain of individual subjects performing a cognitive task, thus providing a starting point for investigating the underlying neural mechanisms. As briefly discussed in the next section, some of these mechanisms, both structural and dy-

namic, can already be inferred or postulated on the basis of phenomenological observations as well as of large-scale computer simulations.

### Possible Structural and Functional Determinants of Clustering

Since neurons must be active in order to be interactive, a functional cluster will in general be constituted by brain regions that are active. Any pathological change in activity is thus expected to affect the composition and strength of a functional cluster. In many cases, however, neural activity and interactivity can be dissociated. This could be due to structural factors. The organization of the anatomical connectivity of certain brain regions, for example the reciprocal connectivity within the thalamocortical system, is well-suited to generating coherent dynamical states (Lumer *et al.*, 1997a,b), while that of other brain regions, for example the cerebellum, may not be as well suited. Structural factors could also be responsible for a dissociation between activity and interactivity in pathological conditions. In split brain patients, the absence of direct, fast interactions between the two hemispheres impairs the integration of information between them, although both hemispheres are normally active and can control behavior (Gazzaniga, 1995). In cats, the transection of the corpus callosum impairs the stimulus-induced synchronization of neuronal groups but not their activation (Engel *et al.*, 1991). A similar dissociation between activity and synchronization is observed in strabismic cats (Koenig *et al.*, 1993).

Functional clustering can also arise through purely functional factors, as shown by large-scale simulations (Lumer *et al.*, 1997a). Nonlinear interactions among neuronal groups, such as those mediated by the activation of voltage-dependent connections, can transiently increase the strength of the interactions among a subset of groups, leading to the formation of functional clusters in the thalamocortical system despite the relative continuity of anatomical connectivity. In some cases, active brain regions may form competing clusters through inhibition or desynchronization (Tononi *et al.*, 1992). Some experimental evidence is available for the dynamic formation of functional borders in the visual cortex of the cat. For instance, orthogonal visual stimuli can result in the transient functional grouping and regrouping of the activity of multiple groups of neurons which are alternately correlated or uncorrelated with each other (Engel *et al.*, 1990). The extent and cohesion of functional clustering is also likely to be modified by the activity of neuromodulatory systems, which can affect the strength of neuronal interactions and the likelihood of synchronization (Munk *et al.*, 1996). Such mechanisms could play a role in schizophrenia and dissociative disorders.

Finally, the time scale at which neural interactions

occur is crucial to the occurrence of functional clustering. Over a sufficiently long time scale, all elements of the brain are likely to be functionally connected to some degree. Over the cognitively crucial time scale of a few hundred milliseconds (Blumenthal, 1977), however, only certain brain regions may interact with sufficient speed and strength as to give rise to a functional cluster. As shown by large-scale simulations, reentrant interactions can result in the formation of a cluster of neuronal groups within the thalamocortical system that are transiently but sharply differentiated from surrounding neurons in terms of the strength of their interactions (Lumer *et al.*, 1997a,b). The simulations also show that such functional clusters arise as a result of a phase transition in the dynamic behavior of the system (Lumer *et al.*, 1997b). Below a well defined transition threshold, such a functional cluster collapses. These results suggest that reductions in conduction velocity or in the efficacy of voltage-dependent connections may precipitate the collapse of functional clustering and lead to functional disturbances.

### CONCLUSIONS

In the present article, a functional cluster has been defined as a subset of strongly interactive regions that show distinct boundaries with the rest of the brain. A measure of functional clustering has been introduced, and its applicability tested on a PET data set. Several theoretically relevant questions about the occurrence of functional clustering in the brain are addressable with neuroimaging techniques offering higher temporal resolution. Some of these questions are as follows. For any given task or group of subjects, is there a set of brain regions that interact much more strongly among themselves than with the rest of the brain; i.e., is there a functional cluster? Does the composition of such a functional cluster change depending upon which cognitive activity the subject is engaged in? Are certain brain regions always included or always excluded from such a functional cluster? Can a functional cluster split, or can multiple clusters coexist in a normal subject? Are there pathological conditions that are reflected in abnormalities of functional clustering? While future experiments will certainly be necessary to address these questions, the present analysis on a PET data set suggests that, in principle, the determination of physiological clusters and of pathological changes in cluster arrangement can reliably be achieved.

### APPENDIX 1: ANALYSIS OF A SAMPLE SYSTEM

For a simple example that demonstrates the properties of the proposed cluster index, consider a system consisting of six binary units,  $\{u_j\}$ , in which the  $j$ th unit can be in one of two states:  $u_j = 0$  or  $u_j = 1$ . This system

is such that  $u_1$ ,  $u_2$ ,  $u_4$ , and  $u_5$  each randomly occupy either state with equal probability  $P = 0.5$ . The state of  $u_3$  is given by the exclusive or (XOR) of  $u_1$  and  $u_2$ ; that is,  $u_3 = u_1 \text{ XOR } u_2$ , and  $u_6 = u_4 \text{ XOR } u_5$ . Hence the system consists by design of two mutually independent functional clusters of 3 units each. All 16 possible states of the system are listed in Table 2.

Each state of this system occurs with equal likelihood. Hence the list of states in the table can be taken as a representative sample of a population of 16 measurements on the system. Notice two properties of the table. First, units 3 and 6 each occupy the 0 and 1 states with equal probability despite their functional association with two other units each. Second, there is zero correlation between all pairs of units (rows of the table). The absence of linear correlations is due to the nonlinear nature of the relation between the units, which is manifest in the alternative mathematical expression  $u_3 = 1 - (u_1 + u_2 - 1)^2$ .

Any clustering technique based on pairwise correlations as a distance metric would thus detect no functional groupings within this system. Clustering techniques based on grouping the measurements together in the six-dimensional space defined by the values of each unit also fail. In fact, standard clustering techniques such as hierarchical agglomerative algorithms as well as partitioning algorithms ( $k$ -means) failed to detect the structure inherent in this system. For instance, the  $k$ -means algorithm ( $k = 2$ ) produced arbitrary bipartitionings determined exclusively by the ordering of the elements. All of these partitionings were equivalent, with  $F = 1$ .

From the known probability distribution of this system or an estimation of it from experimental data, it is possible to calculate the entropies of the system and its various subsets, and then to calculate the derived quantities of integration and mutual information. The entropy of a system with  $M$  discreet states with probabilities  $\{p_j\}$  is  $H = -\sum_{j=1}^M p_j \log p_j$ . For the binary system under consideration, it will be convenient to use the base-2 logarithm. Hence the entropy of a single unit  $u_i$  is just  $H(u_i) = -2 \cdot 0.5 \cdot \log_2 0.5 = \log_2 2 = 1$ . In general, the entropy of any system consisting of  $M$  states each of equal probability  $p = 1/M$  is just  $\log_2 M$ . The entropy of the system consisting of units 1, 2, and 3 is  $H(u_1, u_2, u_3) = \log_2 4 = 2$ , the same as that of units 4,

5, and 6, and the entropy of any other combination of three units is  $\log_2 8 = 3$ . The entropy of the entire system is  $H(u_i) = \log_2 16 = 4$ .

The mutual information between two systems (or subsets of a system) is just the difference between the summed entropies of the two individual systems and the entropy of the combined systems considered together (Eq. (1) in the main text) and reflects the degree to which the two systems are statistically dependent. The integration of a system is a generalization of this measure, defined as the difference between the summed entropies of all individual elements in the system and the entropy of the entire system (Eq. (2)). It reflects the degree to which all elements of the system are statistically dependent. The cluster index defined in the main text (Eq. (3)) captures both of these measures for a particular subset  $X_i$  via the ratio of its integration to its mutual information with the remainder of the system:  $CI(X_i) = I(X_i)/MI(X_i; X - X_i)$ .

In order to determine the cluster indices for the sample system, it is necessary only to consider one example of each type of subset partitioning having a distinct probability distribution function. Table 3 lists each unique subset type. All possible partitionings of the system are equivalent to one of these (for example,  $u_1, u_2, u_3$  also represents  $u_4, u_5, u_6$ ). For each subset the table indicates its integration, its mutual information with the remainder of the system, and the ratio of these two quantities, or the cluster index. Cluster indices of 0 simply reflect the fact that certain subsets have zero integration. A cluster index of 1 indicates the statistical dependence within a subset is equal in magnitude to its dependence with respect to the remainder of the system. Thus a homogeneous system, in which all units are interconnected on average with the same strength, would yield a population of cluster indices around one. Note that only one subset,  $u_1, u_2$ , and  $u_3$ , equivalent to  $u_4, u_5$ , and  $u_6$ , yields a cluster index greater than 1. In this simplified case the cluster index is infinite; in a finite sampling of this system, large but finite values would be obtained on average. Thus the cluster index accurately identifies the two distinct functional entities, even in the absence of pairwise correlations.

In general, the calculation of entropy requires the actual probability distribution of a system or its estimated value from a finite data set. If the data are continuous, the entropy is given by the  $N$ -dimensional integral  $H(X) = -\int_{-\infty}^{\infty} p(\mathbf{x}) \ln p(\mathbf{x}) d\mathbf{x}$ , where  $\mathbf{x}$  is the vector of state values of each of the  $N$  units of the system. If  $p(\mathbf{x})$  cannot be adequately measured, a model distribution which can be fully characterized from a few measurable parameters is often taken as a reasonable approximation to the underlying distribution, as is done in the main text with a multidimensional Gaussian distribution.

TABLE 2

States of the Sample System

|        |   |   |   |   |   |   |   |   |   |   |   |   |   |   |   |   |
|--------|---|---|---|---|---|---|---|---|---|---|---|---|---|---|---|---|
| Unit 1 | 1 | 1 | 1 | 1 | 0 | 0 | 0 | 0 | 1 | 1 | 1 | 1 | 0 | 0 | 0 | 0 |
| Unit 2 | 1 | 1 | 1 | 1 | 0 | 0 | 0 | 0 | 0 | 0 | 0 | 0 | 1 | 1 | 1 | 1 |
| Unit 3 | 0 | 0 | 0 | 0 | 0 | 0 | 0 | 0 | 1 | 1 | 1 | 1 | 1 | 1 | 1 | 1 |
| Unit 4 | 1 | 0 | 1 | 0 | 1 | 0 | 1 | 0 | 1 | 0 | 1 | 0 | 1 | 0 | 1 | 0 |
| Unit 5 | 1 | 0 | 0 | 1 | 1 | 0 | 0 | 1 | 1 | 0 | 0 | 1 | 1 | 0 | 0 | 1 |
| Unit 6 | 0 | 0 | 1 | 1 | 0 | 0 | 1 | 1 | 0 | 0 | 1 | 1 | 0 | 0 | 1 | 1 |

TABLE 3

| Subset $X_j$              | $I(X_j)$ | $MI(X_j; X - X_j)$ | $CI(X_j)$ |
|---------------------------|----------|--------------------|-----------|
| $u_1, u_2$                | 0        | 1                  | 0         |
| $u_1, u_4$                | 0        | 2                  | 0         |
| $u_1, u_2, u_3$           | 1        | 0                  | $\infty$  |
| $u_1, u_2, u_4$           | 0        | 2                  | 0         |
| $u_1, u_2, u_3, u_4$      | 1        | 1                  | 1         |
| $u_1, u_2, u_4, u_5$      | 0        | 2                  | 0         |
| $u_1, u_2, u_3, u_4, u_5$ | 1        | 1                  | 1         |

## APPENDIX 2: STATISTICS OF THE CLUSTER INDEX

The main text outlines a procedure which utilizes mutual information and integration to determine the structure of statistical clustering in a given imaging data set. To draw meaningful conclusions from this procedure it is necessary to construct a system against which to compare the data set. This system should be chosen to have by definition no statistical clustering but in all other aspects be as similar to the data set as possible. This system is required at two stages in the analysis: first, to provide normalization constants so that subsets of the system can be compared independent of subset size, and second, to provide a valid null hypothesis against which to compare the findings in the data set. Such a system is formed by sampling a multidimensional Gaussian process of homogeneous covariance. Below is a brief review of multidimensional Gaussian statistics and a more detailed description of the statistical procedures outlined in the main text.

Consider a system  $X$  described by the  $M \times N$  matrix of elements  $x_{si}$ . The matrix consists of  $M$  row vectors  $\mathbf{x}_s$ , each of which is drawn from an  $N$ -dimensional Gaussian process with probability distribution function  $p(\mathbf{x})$ ,

$$p(\mathbf{x}) = \frac{1}{[(2\pi)^n |C|]^{1/2}} e^{-\mathbf{x}C^{-1}\mathbf{x}^T/2},$$

where  $C$  is the covariance matrix of the distribution, and  $|C|$  is its determinant. Each of the  $N$  columns forms a column vector  $\mathbf{x}_i$ , each of which is a univariate Gaussian process of zero mean.

The covariance matrix of  $X$  is given by  $\text{COV}(X)_{ij} = (1/M) \sum_{s=1}^M x_{si} x_{sj} = \langle \mathbf{x}_i \cdot \mathbf{x}_j \rangle$ . The average observed  $\text{COV}(X)$  over many sample systems  $X$  will tend toward  $C$ , the covariance characterizing the distribution function. For a system characterized by multidimensional Gaussian statistics, the entropy is just  $H(X) = \ln \sqrt{(2\pi e)^N |\text{COV}(X)|}$ , and the integration of  $X$  is given by  $I(X) = -0.5 \ln |\text{CORR}(X)|$ , where  $\text{CORR}(X)$  is the correlation matrix of  $X$ , that is, the matrix the  $ij$ th off-diagonal element of which is the correlation coefficient between  $\mathbf{x}_i$  and  $\mathbf{x}_j$ .

A system characterizing the null hypothesis of no

clustering must be provided in order to gauge the likelihood of obtaining a given CI if no functional clustering is present. The equivalent "null system" employed in this study was chosen to be statistically homogeneous, i.e., have no statistical clustering, and to have the same size, average total integration, and number of samples as the data system being studied. Such a homogeneous system  $X_H$  is sampled from a multidimensional Gaussian probability distribution characterized by a homogeneous correlation matrix  $C(r)$ , that is, with the same value  $r$  on all offdiagonal elements. This value is uniquely determined by the above conditions and was found by numerical search. The average values of integration and mutual information from 100 such systems were used to provide the homogeneous-system integration and mutual information values in the normalized cluster index calculation.

The cluster indices of system  $X_H$  are distributed by definition around a mean of one for all subset sizes. However, as noted in the main text, the width of the CI distribution differs as a function of subset size. This skews the distribution of the observed maximum CI values in favor of large and small subset sizes ( $k = 2, N - 1$ ). Since the goal is to rank subsets in a manner which is independent of subset size, a Student's  $t$ -like parameter,  $t_{CI}$ , was devised:  $t_{CI} = [CI(X_i^k) - \langle CI(X_H^k) \rangle] / \text{std}(CI(X_H^k))$ . In this expression  $CI(X_i^k)$  is the cluster index of the  $i$ th system of subset size  $k$ ,  $\langle CI(X_H^k) \rangle$  is the mean of the cluster-index distribution at subset size  $k$  accumulated from many (here, 100) sampled equivalent homogeneous systems, and  $\text{std}()$  is the standard deviation of the distribution. This parameter was found to remove effectively the asymmetry between subset sizes and was utilized to provide a relative ranking of all subsets according to significance of clustering.

In order to test the significance of CI values, null-hypothesis statistics were generated via Monte Carlo simulations of the same homogeneous systems  $X_H$  as used to provide the normalization constants. This was done by generating  $N$  independent processes  $\mathbf{y}_i$ , each of which consisted of a vector of  $M$  samples drawn from a univariate Gaussian process of zero mean and unit variance. The multidimensional system  $X_H$  was then generated via the linear model  $\mathbf{x}_i = b\mathbf{y}_i + a\sum_{j \neq i} \mathbf{y}_j$ , where  $a = [(N - 2)r + 2 - 2[(1 - N)r^2 + (N - 2)r + 1]^{1/2}]^{1/2}/N$  and  $b = [1 - (N - 1)a^2]^{1/2}$ . The values  $b$  and  $a$  were obtained by solving the equations  $\langle \mathbf{x}_i \cdot \mathbf{x}_j \rangle \equiv r_{ij}$ , setting  $r_{ij} = r$  for  $i \neq j$  and  $r_{ij} = 1$  for  $i = j$ , given the fact that  $\langle \mathbf{y}_i \cdot \mathbf{y}_j \rangle = 0$  for  $i \neq j$  and 1 for  $i = j$ . This is a special case of the general procedure for generating multivariate Gaussian deviates of any given correlation matrix (Rubinstein, 1981). The processes  $\mathbf{x}_i$  will on average have correlation matrix  $C(r)$ , i.e.,  $\langle \text{CORR}(X_H) \rangle = C(r)$ .

The CI calculation was performed and the cluster indices histogrammed for 1000 null systems  $X_H$  in order to provide a confidence level of  $P < 0.001$  (probability of

having obtained a cluster index of a given or larger magnitude from the equivalent homogeneous system). This provides the equivalent of a Bonferroni correction, required since the data set CIs were searched for a maximum, invoking the problem of multiple comparisons. The maximum value observed from all such systems was used as the significance threshold.

## ACKNOWLEDGMENTS

We thank Dr. Shitij Kapur for kindly providing the PET data used for this study. The work performed at The Neurosciences Institute was supported by the Neurosciences Research Foundation. The Foundation received support for this work from Novartis Pharmaceutical Corporation.

## REFERENCES

- Arabie, P., Hubert, L. J., and De Soete, G. 1996. *Clustering and Classification*. World Scientific, Singapore.
- Bleuler, E. 1911 *Dementia praecox or the group of schizophrenias*. International University Press, New York. [English edition 1950]
- Blumenthal, A. L. 1977. *The Process of Cognition*. Prentice-Hall, Englewood Cliffs, NJ.
- Bock, H.-H. 1996. Probability models and hypothesis testing in partitioning cluster analysis. In *Clustering and Classification* (P. Arabie, L. J. Hubert, G. DeSoete, Eds.), pp. 377–453. World Scientific, New Jersey.
- Budinger, T. F. 1992. Critical review of PET, SPECT, and neuroreceptor studies in schizophrenia. *J. Neural Transm.* **36**:3–12.
- Chandon, J.-L., and Pinson, S. 1981. *Analyse Typologique. Theories et Applications*. Masson, Paris.
- Chang, W. C. 1983. On using principal components before separating a mixture of multivariate normal distributions. *Appl. Stat.* **32**:267–275.
- Cormack, R. M. 1971. A review of classification. *J. R. Stat. Soc. A* **134**:321–367.
- Cox, T. F., and Cox, M. A. A. 1994. *Multidimensional Scaling*. Chapman and Hall, London.
- Edelman, G. M. 1987. *Neural Darwinism*. Basic Books, New York.
- Edelman, G. M. 1989. *The Remembered Present*. Basic Books, New York.
- Edgington, E. S. 1980. *Randomization Tests*. Dekker, New York.
- Engel, A. K., König, P., Kreiter, A. K., and Singer, W. 1991. Interhemispheric synchronization of oscillatory neuronal responses in cat visual cortex. *Science* **252**:1177–1179.
- Engel, A. K., König, P., and Singer, W. 1990. Direct physiologic evidence for scene segmentation by temporal coding. *Proc. Natl. Acad. Sci. USA* **88**:9136–9140.
- Everitt, B. S. 1993. *Cluster Analysis*, 3rd ed. Edward Arnold, London.
- Friston, K. J. 1994. Functional and effective connectivity: A synthesis. *Hum. Brain Mapp.* **2**:56–78.
- Friston, K. J., Ashburner, J., Poline, J. B., Frith, C. D., Heather, J. D., and Fracowiak, R. S. J. 1995a. Spatial realignment and normalization of images. *Hum. Brain Mapp.* **2**:165–189.
- Friston, K. J., Holmes, A. P., Worsley, K. J., Poline, J.-P., Frith, C. D., and Fracowiak, R. S. J. 1995b. Statistical parametric maps in functional neuroimaging: A general linear approach. *Hum. Brain Mapp.* **2**:189–210.
- Friston, K. J., and Frith, C. D. 1995. Schizophrenia: A disconnection syndrome? *Clinical Neuroscience* **3**:89–97.
- Friston, K. J., Frith, C. D., Fletcher, P., Liddle, P. E., and Fracowiak, R. S. J. 1996a. Functional topography: Multidimensional scaling and functional connectivity in the brain. *Cerebral Cortex* **6**:156–164.
- Friston, K. J., Tononi, G., Sporns, O., and Edelman, G. M. 1996b. Characterizing the complexity of neural interactions. *Hum. Brain Mapping* **3**:302–314.
- Gazzaniga, M. S. 1995. Principles of human brain organization derived from split-brain studies. *Neuron* **14**:217–28.
- Geschwind, N. 1965. Disconnection syndromes in animals and man. *Brain* **88**:237–294, 585–644.
- Goldberg, G., Podreka, T., Suess, E., and Deecke, L. 1989. The cerebral localization of neuropsychological impairment in Alzheimer's disease: A SPECT study. *J. Neurol.* **236**:131–138.
- Gordon, A. D. 1980. *Classification*. Chapman and Hall, London.
- Heiss, W.-D., Pawlik, G., Holthoff, V., Kessler, J., and Szelies, B. 1992. PET correlates of normal and impaired memory functions. *Cerebrovas. Brain Metab. Rev.* **4**:1–27.
- Jones, D. S. 1979. *Elementary Information Theory*. Oxford Univ. Press, Oxford.
- Kaufman, L., and Rousseeuw, P. J. 1990. *Finding Groups in Data*. Wiley, New York.
- König, P., Engel, A. K., Lowel, S., and Singer, W. 1993. Squint affects synchronization of oscillatory responses in cat visual cortex. *Eur. J. Neurosci.* **5**:501–508.
- Leopold, D. A., and Logothetis, N. K. 1996. Activity changes in early visual cortex reflect monkeys' percepts during binocular rivalry. *Nature* **379**:549–553.
- Lumer, E. D., Edelman, G. M., and Tononi, G. 1997a. Neural dynamics in a model of the thalamocortical system. I. Layers, Loops, and the emergence of fast synchronous oscillations. *Cereb. Cortex* **7**:207–227.
- Lumer, E. D., Edelman, G. M., and Tononi, G. 1997b. Neural dynamics in a model of the thalamocortical system. II. The role of neural synchrony tested through perturbations of spike timing. *Cereb. Cortex* **7**:228–236.
- Lynn, S. J., and Rhue, J. W. (Eds.) 1994. *Dissociation: Clinical and Theoretical Perspectives*. Guilford Press, New York.
- McIntosh, A. R., and Gonzalez-Lima, F. 1994. Structural equation modeling and its application to network analysis of functional brain imaging. *Hum. Brain Mapp.* **2**:2–22.
- McIntosh, A. R., Grady, C. L., Ungerleider, L. G., Haxby, J. V., Rapoport, S. I., and Horwitz, B. 1994. Network analysis of cortical visual pathways mapped with PET. *J. Neurosci.* **14**:655–666.
- McIntosh, A. R., Bookstein, F. L., Haxby, J. V., and Grady, C. L. 1996a. Spatial pattern analysis of functional brain images using partial least squares. *Neuroimage* **3**:143–157.
- McIntosh, A. R., Grady, C. L., Haxby, J. V., Ungerleider, L. G., and Horwitz, B. 1996b. Changes in limbic and prefrontal functional interactions in a working memory task for faces. *Cerebral Cortex* **6**:571–584.
- McKeown, M. J., Makeig, S., Brown, G. G., Jung, T.-P., Kindermann, S. S., Bell, A. J., and Sejnowski, T. J. 1997. Analysis of fMRI data by decomposition into independent components. *Neurology* **48**:A417.
- McLaughlin, T., Steinberg, B., Christensen, B., Law, I., Parving, A., and Friberg, L. 1992. Potential language and attentional networks revealed through factor analysis of rCBF data measured with SPECT. *J. Cereb. Blood Flow Metab.* **12**:535–545.
- Moeller, J. R., Strother, S. C., Sidtis, J. J., and Rottenberg, D. A. 1987. Scaled subprofile model: A statistical approach to the analysis of functional patterns in emission tomographic data. *J. Cereb. Blood Flow Metab.* **7**:649–658.
- Munk, M. H., Roelfsema, P. R., Koenig, P., Engel, A. K., and Singer, W.

1996. Role of reticular activation in the modulation of intracortical synchronization. *Science* **272**:271–274.
- Papoulis, A. 1991. *Probability, Random Variables, and Stochastic Processes*, 3rd ed. McGraw-Hill, New York.
- Petersen, S. E., Fox, P. T., Posner, M. I., Mintun, M., and Raichle, M. E. 1988. Positron emission tomographic studies of the cortical anatomy of single-word processing. *Nature* **331**:585–589.
- Rubinstein, R. Y. 1981. *Simulation and the Monte Carlo Method*. Wiley, New York.
- Shannon, C. E., and Weaver, W. 1949. *The Mathematical Theory of Communication*. University of Illinois Press, Chicago.
- Sneath, P. H. A. 1980. The risk of not recognizing from ordinations that clusters are distinct. *Classi. Soc. Bull.* **4**:22–43.
- Tononi, G., Sporns, O., and Edelman, G. M. 1992. Reentry and the problem of integrating multiple cortical areas: Simulation of dynamic integration in the visual system. *Cereb. Cortex* **2**:310–335.
- Tononi, G., Sporns, O., and Edelman, G. M. 1994. A measure for brain complexity: Relating functional segregation and integration in the nervous system. *Proc. Natl. Acad. Sci. USA* **91**:5033–5037.
- Tononi, G., Sporns, O., and Edelman, G. M. 1996. A measure for the selective matching of signals by the brain. *Proc. Natl. Acad. Sci. USA* **93**:3422–3427.
- Tononi, G., and Edelman, G. M. Consciousness and the integration of information in the brain. In *Consciousness* (H. H. Jasper, L. Descarries, V. Castellucci, and S. Rossignol, Eds.). Raven Press, New York.
- Tononi, G., Srinivasan, R., Russell, D. P., and Edelman, G. M. Investigating neural correlates of conscious perception by frequency-tagged neuromagnetic responses. *Proc. Natl. Acad. Sci. USA*, in press.
- Widaman, K. F. 1993. Common factor analysis versus principal components analysis: Differential bias in representing model parameters? *Mult. Behav. Res.* **28**:263–312.